# Bis(2,2′-bipyridine)(1,2-diimino-9,10-anthraquinone)ruthenium(II) Derivatives: A ZINDO Analysis of a Redox Series Involving Coupled Proton and Electron Transfers

**Carlos Jorge da Cunha,[†] Elaine S. Dodsworth,[‡] Mario Artur Monteiro,[‡] and A. B. P. Lever*[,‡]**

Department of Chemistry, York University, Toronto, Ontario, Canada M3J1P3, and Depto. de Quimica, Universidade Federal do Paraná, Brazil

*Received May 19, 1999*

The complex bis(2,2′-bipyridine)(1,2-diimino-9,10-anthraquinone)ruthenium(II) can be reduced or oxidized in protic or aprotic media generating various species. The first two reduced species in protic medium and the first two reduced species in aprotic medium were studied by electrochemistry, spectroelectrochemistry, and electronic, NMR, EPR, and infrared spectroscopy and identified as containing different redox/protonation states of the anthraquinone ligand. The ZINDO method was employed to assign electronic transitions and predict their energies. The extent of electronic coupling between the metal and ligand centers was deduced from the ZINDO analysis as a function of net oxidation state and proton complement.

## 1. Introduction

We have been especially interested in the structural characterization, electrochemistry, spectroscopy, magnetic properties, and electronic structure of redox series of transition-metal complexes involving noninnocent quinone-related ligands,[1−18] being a field which has evinced considerable interest; e.g. see refs 19−37.

We have discussed the physical properties of a series of bis-(2,2′-bipyridine)ruthenium(II) complexes containing quinonoid ligands involving a redox series based upon the reduced catecholate (O.O), *o*-aminophenolate ($NH_m$.O), *o*-aminothiophenolate ($NH_m$.S), and quinone diamine ($NH_m$.$NH_m$) species where the coordinating atoms are shown in parentheses. The metal center can exist in the $Ru^{II}$ or $Ru^{III}$ oxidation states, the 2,2′-bipyridine (bpy) ligand can be reduced, and the quinonoid ligands have three redox forms, the fully reduced catechol ($catH_m$) (actually an −NH analogue of catechol), the partially oxidized semiquinone ($sqH_m$), and the fully oxidized quinone ($qH_m$). The subscript m indicates the number of protons attached to the donor atoms in each species. In principle, the catechol

[†] Universidade Federal do Paraná.
[‡] York University.

(1) Masui, H.; Lever, A. B. P.; Auburn, P. R. *Inorg. Chem.* **1991**, *30*, 2402.
(2) Haga, M. A.; Lever, A. B. P.; Dodsworth, E. S. *J. Am. Chem. Soc.* **1986**, *108*, 7413.
(3) Del Medico, A.; Fielder, S. S.; Lever, A. B. P.; Pietro, W. J. *Inorg. Chem.* **1995**, *34*, 1507.
(4) Haga, M. A.; Dodsworth, E. S.; Lever, A. B. P. *Inorg. Chem.* **1986**, *25*, 447.
(5) Auburn, P. R.; Dodsworth, E. S.; Haga, M. A.; Liu, W.; Nevin, W. A.; Lever, A. B. P. *Inorg. Chem.* **1991**, *30*, 3502.
(6) Tse, Y. H.; Auburn, P. R.; Lever, A. B. P. *Can. J. Chem.* **1992**, *70*, 1849.
(7) Metcalfe, R. A.; Lever, A. B. P. *Inorg. Chem.* **1997**, *36*, 4762.
(8) Metcalfe, R. A.; Dodsworth, E. S.; Fielder, S. S.; Stufkens, D. J.; Lever, A. B. P.; Pietro, W. J. *Inorg. Chem.* **1996**, *35*, 7741.
(9) Metcalfe, R. A.; Dodsworth, E. S.; Lever, A. B. P.; Pietro W. J.; Stufkens, D. J. *Inorg. Chem.* **1993**, *32*, 3581.
(10) Delmedico, A.; Auburn, P. R.; Dodsworth, E. S.; Lever, A. B. P.; Pietro, W. J. *Inorg. Chem.* **1994**, *33*, 1583.
(11) Masui, H.; Lever, A. B. P.; Dodsworth, E. S. *Inorg. Chem.* **1993**, *32*, 258.
(12) Masui, H.; Ph.D. Dissertation, York University, Toronto, Ontario, Canada, 1994; p 158.
(13) Metcalfe, R. A.; Vasconcellos, L. C. G.; Mirza, H.; Franco, D. W.; Lever, A. B. P. *J. Chem. Soc., Dalton Trans.*, submitted for publication.
(14) da Cunha, C. J.; Fielder, S. S.; Stynes, D. V.; Masui, H.; Auburn. P. R.; Lever, A. B. P. *Inorg. Chim. Acta* **1996**, *242*, 293.
(15) Ebadi, M.; Lever, A. B. P. *Inorg. Chem.* **1999**, *38*, 0000.
(16) Del Medico, A.; Pietro, W. J.; Lever, A. B. P. *Inorg. Chim. Acta* **1998**, *281/2*, 126.
(17) Lever, A. B. P.; Auburn, P. R.; Dodsworth, E. S.; Haga, M. A.; Liu, W.; Melnik, M.; Nevin, W. A. *J. Am. Chem. Soc.* **1988**, *110*, 8076.
(18) Masui, H.; Freda, A. L.; Lever, A. B. P. *Inorg. Chem.*, submitted for publication.
(19) Heinze, K.; Huttner, G.; Zsolnai, L.; Jacobi, A.; Schober, *P. Chem. Eur. J.* **1997**, *3*, 732.
(20) Jung, O. S.; Jo, D. H.; Park, S. H.; Sohn, Y. S. *Bull. Korean Chem. Soc.* **1997**, *18*, 628.
(21) Kondo, M.; Hamatani, M.; Kitagawa, S.; Pierpont, C. G.; Unoura, K. *J. Am. Chem. Soc.* **1998**, *120*, 455.
(22) Lange, C. W.; Pierpont, C. G. *Inorg. Chim. Acta* **1997**, *263*, 219. Pierpont, C. G.; Buchanan, R. M. *Coord. Chem. Rev.* **1981**, *38*, 45. Pierpont, C. G.; Lange, C. W. *Pure Appl. Chem.* **1994**, *41*, 331. Pierpont, C. G.; Larsen, S. K.; Boone, S. R. *Pure Appl. Chem.* **1988**, *60*, 1331.
(23) Lee, K. K. H.; Wong, W. T. *J. Organomet. Chem.* **1997**, *547*, 329.
(24) Paw, W.; Eisenberg, R. *Inorg. Chem.* **1997**, *36*, 2287.
(25) Ruf, M.; Noll, B. C.; Groner, M. D.; Yee, G. T.; Pierpont, C. G. *Inorg. Chem.* **1997**, *36*, 4860.
(26) Temme, O.; Laschat, S.; Frohlich, R.; Wibbeling, B.; Heinze, J.; Hauser, P. *J. Chem. Soc., Perkin Trans. 2* **1997**, 2083.
(27) Attia, A. S.; Bhattacharya, S.; Pierpont, C. G. *Inorg. Chem.* **1995**, *34*, 4427.
(28) Attia, A. S.; Conklin, B. J.; Lange, C. W.; Pierpont, C. G. *Inorg. Chem.* **1996**, *35*, 1033.
(29) Jung, O. S.; Jo, D. H.; Lee, Y. A.; Conklin, B. J.; Pierpont, C. G. *Inorg. Chem.* **1997**, *36*, 19.
(30) Jung, O. S.; Jo, D. H.; Lee, Y. A.; Sohn, Y. S.; Pierpont, C. G. *Angew. Chem., Int. Ed. Engl.* **1996**, *35*, 1694.
(31) Jung, O. S.; Lee, Y. A.; Pierpont, C. G. *Synth. Met.* **1995**, *71*, 2019. Pierpont, C. G.; Jung, O. S. *Inorg. Chem.* **1995**, *34*, 4281.
(32) Keyes, T. E.; Forster, R. J.; Jayaweera, P. M.; Coates, C. G.; McGarvey, J. J.; Vos, J. G. *Inorg. Chem.* **1998**, *37*, 5925.
(33) Speier, G.; Csihony, J.; Whalen, A. M.; Pierpont, C. G. *Inorg. Chim. Acta* **1996**, *245*, 1.
(34) Speier, G.; Whalen, A. M.; Csihony, J.; Pierpont, C. G. *Inorg. Chem.* **1995**, *34*, 1355.
(35) Haga, M.; Isobe, K.; Boone, S. R.; Pierpont, C. G. *Inorg. Chem.* **1990**, *29*, 3795.
(36) Ruf, M.; Noll, B. C.; Groner, M. D.; Yee, G. T.; Pierpont, C. G. *Inorg. Chem.* **1997**, *36*, 4860.
(37) Gutlich, P.; Dei, A. *Angew. Chem., Int. Ed. Engl.* **1998**, *36*, 2734.

10.1021/ic9905594 CCC: $18.00 
Published on Web 10/28/1999

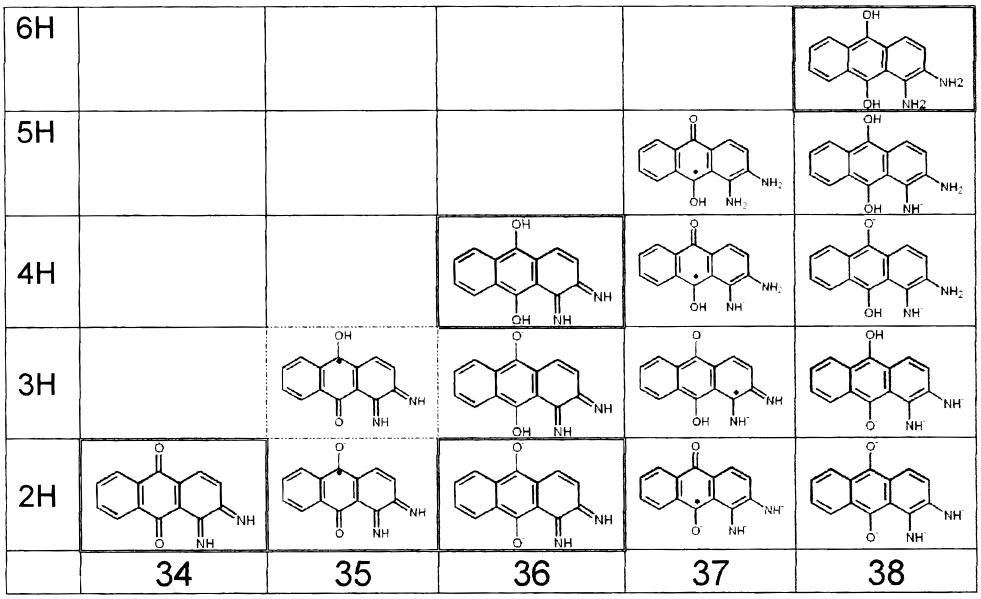


**Figure 1.** Molecular structures of one tautomer of each selected redox/protonation states of the DAAQ system. Each of the 3H, 4H, and 5H species has four isomers (see Figure 2 for 36−4H). The species detected in this work as $[Ru(bpy)_2(LL)]^{2+}$complexes are boxed in double lines.

species can exist in protonated ($m = 2$) or deprotonated ($m = 1$) forms, and these have been observed for all the above-described systems with the exception of (O.O) where the coordinated protonated form has not yet been identified in the $[Ru(bpy)_2]^{2+}$ series.

We have recently published[14] the preparation, characterization, X-ray structure, and a description of the electronic structure of $[Ru(bpy)_2(DIAQ)]^{2+}$, where the benzoquinonediimine (NH,-NH) fragment (I) of 1,2-diiminoanthraquinone (DIAQ) is bound strongly to the $[Ru(bpy)_2]^{2+}$ moiety. It was proposed that the DIAQ ligand is the strongest neutral $\pi$-accepting ligand yet described with very strong coupling between a d$\pi$ orbital of the ruthenium and the lowest $\pi^*$ level of the ligand.

The parent diaminoanthraquinone (DAAQ) ligand has two redox active centers, the 9,10-quinone (O,O) center and the 1,2-diamino (N,N) periphery. Each is capable of existing in three oxidation states with the added complexity that the fully reduced species may be protonated or deprotonated at the oxygen or nitrogen sites.

Thus quinones (q) can be reduced in aprotic media in two consecutive one- electron steps generating a semiquinonate (sq) and a catecholate (cat) species.[38] In protic media the quinones can be reduced in one two-electron, two-proton step generating a catechol ($catH_2$) species. Benzoquinonediimine ($qH_2$) complexes can be reduced in aprotic media in two one-electron steps generating a semiquinonate ($sqH_2$) and a benzodiamide ($catH_2$) complex.[1,3,7,11] In protic media benzoquinonediimine complexes can be reduced in one two-electron two-proton step generating diaminobenzene ($catH_4$) complexes.[7,39] The bpy ligands can also be reduced in various one-electron steps.[40]

The $[Ru(bpy)_2$ $DIAQ]^{2+}$ complex combines quinone, benzoquinonediimine, ruthenium, and bpy fragments and hence displays a rich, proton-dependent electrochemistry. Further, many of the species can exist in a range of tautomeric forms.

The various redox−protonation states of DAAQ can be seen in Figure 1. The labels of each state contain the number of valence electrons (34, 35, 36, 37, or 38) not involved in skeletal $\sigma$-bonding with the carbon atoms and also the number of protons (2H, 3H, 4H, 5H, or 6H) bound to nitrogen and/or oxygen atoms. Thus DIAQ is 34−2H, and DAAQ is 36−4H. The structures were built by assuming metal coordination on the NH.NH site, and in cases where more than one structure is possible the most likely form is shown (see below). Complexes with 3H, 4H, or 5H have four possible isomers; those of 36−4H are shown in Figure 2.

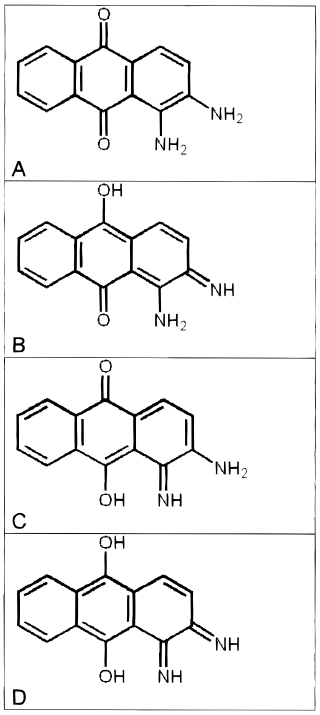


**Figure 2.** Molecular structures of four tautomers of the species $[Ru(bpy)_2(36-4H)]^{2+}$.

Two complexes generated by reduction of the parent $[Ru(bpy)_2(34-2H)]^{2+}$ species in aprotic media ($[Ru(bpy)_2(35-2H)]^{+}$ and $[Ru(bpy)_2(36-2H)]$ ) and two complexes generated by reduction in protic media ($[Ru(bpy)_2(36-4H)]^{2+}$ and $[Ru(bpy)_2(38-6H)]^{2+}$) were identified spectroscopically, the [36−

(38) Patai, S., Ed. *The Chemistry of Quinonoid Compounds*; John Wiley: New York, 1974; Vol. 1.
(39) Brown, G. M.; Weaver, T. R.; Keene, F. R.; Meyer, T. J. *Inorg. Chem.* **1976**, *15*, 190.
(40) Vlcek, A. A. *Coord. Chem. Rev.* **1982**, *43*, 39.

4H] and [35−2H] species also being isolated. One oxidized complex containing $Ru^{III}$ and two reduced forms of the free ligand (37−4H, 38−4H) were detected electrochemically. The general label LL will be used to designate the parent ligand fragment DIAQ when the redox/protonation level is undefined or where we wish to comment in a general fashion. The electronic spectra of the five $[Ru(bpy)_2(LL)]^{n+}$ complexes were assigned according to molecular orbital diagrams based on a ZINDO analysis.

The objectives of the research were to characterize many members of this redox/protonation series, to assign their electronic spectra, and through ZINDO analyses, to determine how the electronic coupling of the ruthenium to the ligand was influenced by the number of electrons and protons. We also required to make comparisons with simpler parent benzoquinonediimine species. In addition to back-donation to ligand $\pi^*$-levels, mixing between metal d$\pi$ and ligand $\pi$-levels is very important in some of the species.

## 2. Experimental Section

**2.1. Reagents and Materials.** Acetonitrile (Caledon) and dichloroethane (Caledon) were distilled from $P_2O_5$, and methanol (Caledon) was dried over 3 Å molecular sieves prior to use in electrochemical or spectroscopic measurements. Water was doubly distilled and passed through Barnstead activated charcoal and ion-exchange resin. Zinc amalgam was prepared in our laboratories by standard procedures. The following reagents were used as supplied: acetone-$d_6$ (Sigma 99.5 at. %), $SnCl_2 \cdot 2H_2O$, (AnalaR), $NH_4PF_6$ (Aldrich), HCl (Caledon), $H_2SO_4$ (Fisher), NaOH (AnalaR), tetrabutylammonium hexafluorophosphate ($(TBA)PF_6$) (Fluka), sodium acetate (Anachemia), ferrocene (Aldrich), and methanol (Caledon) for use in synthesis.

**2.2. Physical Methods.** For electrochemistry, Princeton Applied Research models 173, 174, and 179 and an XY recorder were used as well as a computer-controlled Cypress System (software version 5.5). Cyclic voltammograms were obtained at platinum working and counter electrodes in dry acetonitrile solutions containing 0.1 M $(TBA)PF_6$. An AgCl-coated silver wire, separated from the bulk solution by a frit, served as reference electrode, and ferrocene was added as an internal reference. Potentials were reported versus SCE assuming the ferrocenium/ferrocene couple to be at 0.425 V versus SCE.[41]

UV/vis/NIR spectroscopic data were collected using a Hewlett-Packard HP 8452A diode array or a Varian Cary 2400 spectrometer. Electron spin resonance data were collected with a Varian model E4, while FTIR data were collected with a Nicolet SX20. NMR data were obtained using a Bruker ARX 400 MHz spectrometer.

Each NMR spectrum of complex $[Ru(bpy)_2(36-4H)]^{2+}$ was recorded in acetone-$d_6$ solution (10 mg/0.5 mL) at room temperature. One-dimensional (1D) and two-dimensional (2D) $^1H$ NMR experiments were performed in the Fourier transform mode. The 2D experiments were performed with the following parameters: $^1H-^1H$ COSY [512 × 1024 data matrix, zero-filled to 1024 data points in t1, spectral width of 2008 Hz, 16 scans per t1 value, 1.0 or 1.5 s for the recycle delay, unshifted sine-bell filtering in t1 and t2 for COSY] and shifted sine-squared filtering in t1 and t2 for $^1H-^1H$ NOESY [256 × 2058 data matrix, zero-filled to 1024 data points in t1, 32 scans per t1 value, recycle delay of 2.0 s, and mixing time of 250 ms]. The acetone proton resonance at 2.07 ppm versus TMS was used as a reference.

**2.3. Synthesis.** All steps were performed under an argon atmosphere unless otherwise specified. The preparation of $[Ru(bpy)_2(34-2H)](PF_6)_2$ has been described.[14]

**2.3.1. Synthesis of $[Ru(bpy)_2(36-4H)](PF_6)_2$.** The complex $[Ru(bpy)_2(34-2H)](PF_6)_2$ (0.1 mmol, 93.9 mg) was dissolved in 50 mL of HCl (0.1 M in methanol) to give a purple solution. Solid $SnCl_2 \cdot 2H_2O$ (1 mmol, 225.6 mg) was added with stirring resulting in the rapid generation of a green color. The air and heat sensitive green solution was concentrated at room temperature on a rotary evaporator to 10 mL, and a methanolic saturated solution of $NH_4PF_6$ (1 mmol, 163 mg) was added. Slow addition of ether induced the precipitation of a green solid, which was then isolated by filtration. The air and heat sensitive green complex was characterized spectroscopically as $[Ru(bpy)_2(36-4H)]^{2+}$. In acetone solution (under argon) at room temperature the green complex can be kept for up to 5 h without noticeable change. In acetonitrile, dichloroethane or water the green complex immediately reacts.

**2.3.2. Synthesis of $[Ru(bpy)_2(35-2H)](PF_6)$.** $[Ru(bpy)_2(34-2H)](PF_6)_2$ (93.9 mg, 0.1 mmol) was dissolved in 2 mL of a methanolic solution of triethylamine (0.1 M/L). The brown cationic species so formed is precipitated as the hexafluorophosphate salt by the addition of diethyl ether. Filtration followed by washing with a methanol/ether mixture (10/90) and air-drying gave the complex in 80% yield. Anal. Calcd for $[Ru(bpy)_2(35-2H)](PF_6) \cdot H_2O$, $C_{34}H_{26}F_6N_6O_3PRu$: C, 50.25; H, 3.22; N, 10.34. Found: C, 50.1; H, 3.4; N, 10.35.

For in-situ generation of this species, 1 $\mu$mol (0.939 mg) of $[Ru(bpy)_2(34-2H)](PF_6)_2$ was dissolved in NaOH (10 mL, 0.001 M in methanol) to yield a yellowish-brown solution identified as $[Ru(bpy)_2(35-2H)]^+$. The yellowish-brown color slowly disappears giving a pink solution of as yet unknown composition.

**2.3.3. Chemical Generation of $[Ru(bpy)_2(38-6H)]^{2+}$.** Complex $[Ru(bpy)_2(34-2H)]^{2+}$ (1 $\mu$mol, 0.939 mg) was dissolved in sulfuric acid (1 M in methanol) giving a purple solution; Zn(Hg) was added with vigorous stirring until a yellow color developed. The yellow complex was spectroscopically identified as the complex $[Ru(bpy)_2(38-6H)]^{2+}$.

**2.3.4. Chemical Generation of $[Ru(bpy)_2(36-2H)]$.** A 1 $\mu$mol (0.939 mg) amount of $[Ru(bpy)_2(36-4H)](PF_6)_2$ was dissolved in 10 mL of methanol, and NaOH (saturated in methanol) was added until the color changed from green to yellow.

**2.3.5. Electrochemical generation of $[Ru(bpy)_2(35-2H)]^+$ and $[Ru(bpy)_2(36-2H)]$.** The complex $[Ru(bpy)_2(34-2H)](PF_6)_2$ (5 $\mu$mol, 4.695 mg) was dissolved in dichloroethane or acetonitrile (5 mL containing 0.1 M $(TBA)PF_6$) and loaded into a spectroelectrochemical Hartl cell.[11,42] The complexes $[Ru(bpy)_2(35-2H)]^+$ and $[Ru(bpy)_2(36-2H)]$ could then be generated by controlled potential electrolysis. The same experiment was done in methanol (0.1 M sodium acetate), but under these conditions the complex $[Ru(bpy)_2(34-2H)]^{2+}$ is partially reduced by the solvent to $[Ru(bpy)_2(35-2H)]^+$.

**2.4. ZINDO Optimization and Electronic Spectra Derivation.** The structures of the various closed-shell complexes were derived using restricted Hartree−Fock (RHF) theory and the modified INDO/1 semiempirical method ZINDO/1, while electronic spectra were derived using ZINDO/S[43−51] (Hyperchem program v 4.5 and, later, v5.1, Hypercube Inc., Gainesville, FL). RHF calculations were carried out on Pentium and Pentium II PCs. The open-shell $[Ru(bpy)_2(35-2H)]^+$ species was optimized and spectra derived using INDO/ROHF theory on a Silicon Graphics Unix platform using code written by Prof. M. C. Zerner.

Convergence was assumed when the gradient was lower than about 30 cal $mol^{-1}$ $Å^{-1}$. Scaling parameters were $k_{p\sigma} = 1$ and 1.267 and $k_{p\pi} = 1$ and 0.585 for ZINDO/1 and ZINDO/S, respectively. Small variations in these parameters had no significant effect on the

(41) Lever, A. B. P.; Speier, G.; Milaeva, E. R. *Phthalocyanines: Properties and Applications*; Leznoff, C. C., Lever, A. B. P., Eds.; VCH: New York, 1993; Vol. 3, p 1.
(42) Krejcik, M.; Danek, M.; Hartl, F. *J. Electroanal. Chem.* **1991**, *317*, 179.
(43) Bacon, A. D.; Zerner, M. C. *Theor. Chim. Acta* **1979**, *53*, 21.
(44) Zerner, M. C. *Metal-Ligand Interactions;* Kluwer Academic Publishers: Dordrecht, The Netherlands, 1996; p 493.
(45) Zerner, M. C.; Loew, G. H.; Kirchner, R. F.; Mueller-Westerhoff, U. T. *J. Am. Chem. Soc.* **1980**, *102*, 589.
(46) Culberson, J. C.; Knappe, P.; Rösch, N.; Zerner, M. C. *Theor. Chim. Acta* **1987**, *71*, 21.
(47) Ridley, J.; Zerner, M. C. *Theor. Chim. Acta*, **1973**, *32*, 111.
(48) Ridley, J.; Zerner, M. C. *Theor. Chim. Acta* **1976**, *42*, 223.
(49) Anderson, W. P.; Cundari, T.; Drago, R. S.; Zerner, M. C. *Inorg. Chem.* **1989**, *29*, 1.
(50) Anderson, W. P.; Cundari, T.; Zerner, M. C. *Int. J. Quantum Chem.* **1991**, *39*, 31.
(51) Anderson, W. P.; Edwards, W. D.; Zerner, M. C. *Inorg. Chem.* **1986**, *25*, 2728.

**Table 1.** Selected Bond Distances in ZINDO/1 Optimized Structures Used for Computation (pm)

| bond | 34−2H | 35−2H | 36−2H | 36−4H | 38−6H |
|---|---|---|---|---|---|
| Ru−N(bpy) | 206 | 204 | 203 | 203 | 204 |
| Ru−N(LL) | 205, 203 | 204, 202 | 205, 203 | 205, 204 | 209 |
| C−N(LL) | 133 | 137,139 | 133 | 133 | 143 |
| C−O(LL) | 121 | 127 | 128,130 | 138, 137 | 139, 137 |

calculations, but the common alternative $\pi-\pi$ overlap weighting factor ($k_{p\pi} = 0.64$) yielded somewhat poorer agreement with the observed electronic spectra. The ruthenium bases of Krogh-Jespersen[52] were employed, but for ZINDO/1 using Ru, $\beta(4d) = -20$ eV, which yielded better agreement with X-ray structural data for these complexes.[53] All other parameters used in ZINDO/1 were the default parameters in the Hyperchem program. The ketone C═O bonds optimized at 129 pm and were constrained to 121 pm in the 34−2H complex to agree with X-ray data. The Ru−N(bpy) distances were also constrained to the X-ray values in the 34−2H complex. No restraints were applied to any of the other complexes. Selected bond distances are shown in Table 1. These distances lie in the range anticipated from the previous X-ray literature for complexes of this general class (see more comment below).

The electronic spectra were calculated with configurational interaction at the single excitation level. The number of configurations used was generally 20−25 (occupied orbitals) × 20−25 (unoccupied orbitals). Oscillator strengths were calculated in the dipole length approximation including the one-center sp and pd atomic terms.

## 3. Results and Discussion

Of the complexes shown in Figure 1 physical data were collected for those shown in double outlined boxes, but only those with LL = 34−2H, 35−2H and 36−4H were isolated. We first provide the information which defines each species, the relevant tautomeric form, and the redox and acid/base relationships between them.

The structure of the LL = 34−2H complex has been shown by X-ray crystallography.[14] The complexes $[Ru(bpy)_2(35-2H)]^+$, $[Ru(bpy)_2(36-2H)]$, and $[Ru(bpy)_2(38-6H)]^{2+}$ have only one possible tautomer (Figure 1) whereas complex $[Ru(bpy)_2(36-4H)]^{2+}$ has four possible tautomers (Figure 2). The complexes $[Ru(bpy)_2(35-2H)]^+$, $[Ru(bpy)_2(36-2H)]$, $[Ru(bpy)_2(36-4H)]^{2+}$, and $[Ru(bpy)_2(38-6H)]^{2+}$ were characterized by their electronic spectra and by their mutually consistent electrochemical, coulometric, and acid base behavior (see section 3.4). The $[Ru(bpy)_2(36-4H)]^{2+}$ species was characterized by bidimensional NMR techniques. ZINDO calculations on specific tautomers also provide additional evidence.

The species $[Ru(bpy)_2(38-6H)]^{2+}$ is extremely air sensitive and was not isolated. The absence, in its electronic spectrum, of any low electronic energy absorption attributable to Ru(d$\pi$) → (38−6H) transitions is consistent with the formulation of the ligand in a fully reduced diaminodihydroxoanthracene state.

**3.1. Electrochemistry.** The cyclic voltammogram of [34−2H] {N.B.: henceforth the [···] signifies the $[(bpy)_2Ru]^{2+}$ complex with these species} in acetonitrile (Figure S1) shows a set of reversible couples readily assignable as shown in Table 2, which also shows a comparison of redox potentials, $E_{1/2}$, of [34−2H] with the related free ligands and benzoquinonediimine (bqdi) species.[11] The processes $[Ru(bpy)_2(34-2H)]^{2+}/[Ru(bpy)_2(35-2H)]^+$, $[Ru(bpy)_2(35-2H)]^+/[Ru(bpy)_2(36-2H)]$, and $[Ru(bpy)_2(34-2H)]^{2+}/[Ru(bpy)_2(36-4H)]^{2+}$ were shown to involve one electron, one electron, and two electrons, respectively, by coulometry. The substitution of H atoms 1 and 2 of the anthraquinone free ligand by two amino groups (DAAQ) shifts the q/sq couple 0.16 V more negatively. Replacement of one proton of each amino group of DAAQ by the fragment $[Ru(bpy)_2]^{2+}$ in the complex $[Ru(bpy)_2(34-2H)]^{2+}$ then shifts the q/sq couple 1 V more positively. The sq radical formed is the complex $[Ru(bpy)_2(35-2H)]^+$, and the diamide form is $[Ru(bpy)_2(36-2H)]$.

**Table 2.** Comparative Electrochemical Data, in Acetonitrile, V vs SCE[a]

| species | $Ru^{III/II}$ | q/sq | sq/cat | bpy/bpy$^-$ | ref |
|---|---|---|---|---|---|
| anthraquinone[c] | | −0.83 | −1.44 | | 54 |
| DAAQ[c] | | −0.99 | −1.44 | | tw |
| $[Ru(bpy)_2(34-2H)]^{2+}$ | 1.67 | 0.22 | −0.36 | −1.47, −1.67 | tw |
| $[Ru(bpy)_2(bqdi)]^{2+}$ [b] | 1.37 | −0.45 | −1.13 | −1.70, −1.94 | 11 |

[a] Our data corrected against ferrocene assuming[41] the $Fc^+/Fc$ couple in acetonitrile lies at 0.425 V vs SCE. [b] bqdi = *o*-benzoquinonediimine. [c] Free ligand; tw = this work.

Comparison with the bqdi data shows that the 34−2H ligand is significantly more electron withdrawing[14] than bqdi, with ligand-localized oxidation potentials and the $Ru^{III/II}$ potential being shifted positively.

**3.2. Tautomeric Form of Complex $[Ru(bpy)_2(36-4H)]^{2+}$.**

**3.2.1. NMR Spectra.** Good evidence for the structure of the $[Ru(bpy)_2(36-4H)]^{2+}$ complex was obtained from 1D and 2D COSY NMR data. The one-dimensional $^1H$ NMR spectrum of the complex, recorded in acetone-$d_6$, shows seven clusters of peaks in the region between 7 and 9 ppm and four broad singlet peaks between 9 and 14 ppm that disappear upon addition of $D_2O$ (Supporting Information Figure S2). The spectrum is consistent with [36−4H] isomer D (Figure 2).

The COSY $^1H-^1H$ spectrum of complex [36−4H] was also recorded and can be seen in Figure S3 with the respective assignments of the peaks between 7 and 9 ppm (Table S1). The peaks at 8.0 and 7.2 ppm have a coupling constant *J* of 9.9 Hz typical of cyclic alkenes and are identified with protons 3a and 4a. An $^1H-^1H$ NOESY experiment showed a through space connectivity between the proton at 12.22 ppm (10a) and the protons at 8.48 ppm (5a) and 7.2 ppm (4a), thus unambiguously assigning protons 4a and 3a.

The bpy proton assignments[16,55−61] are in agreement with those made previously on other *cis*-$[Ru(bpy)_2XY]^n$ complexes where the bpy protons H3 and H3′ are more deshielded than protons H4,H4′, which in turn are more deshielded than protons H5,H5′. No specific trend is observed for protons H6,H6′ because their relative positions depend strongly on the nature of the ligand XY.

**3.2.2. FTIR Spectra.** In Figure S4 the FTIR spectrum of complex [36−4H] is compared with that of the well-characterized complex[14] [34−2H]. The following tentative assignments

(52) Krogh Jespersen, K.; Westbrook, J. D.; Potenza, J. A.; Schugar, H. J. *J. Am. Chem. Soc.* **1987**, *109*, 7025.
(53) Gorelsky, S. I.; Lever, A. B. P. Unpublished observations.
(54) Ashnagar, A.; Bruce, J. M.; Dutton, P. L.; Prince, R. C. *Biochim. Biophys. Acta* **1984**, *801*, 351.
(55) Lytle, F. E.; Petrosky, L. M.; Carlson, L. R. *Anal. Chim. Acta* **1971**, *57*, 239.
(56) Hage, R.; Prins, R.; Haasnoot, J. G.; Reedijk, J.; Vos, J. G. *J. Chem. Soc., Dalton Trans.* **1987**, 1389.
(57) Hage, R.; Dijkhnis, A. H. J.; Haasnoot, J. G.; Prins, R.; Reedjik, J.; Buchanan, B. E.; Vos, J. G. *Inorg. Chem.* **1988**, *27*, 2185.
(58) Hitchcock, P. B.; Seddon, K. R.; Turp, J. E.; Yousif, Y. Z.; Zoray, J. A.; Constable, E. C.; Wernberg, O. *J. Chem. Soc., Dalton Trans.* **1988**, 1837. Constable, E. C.; Lewis, J. *Inorg. Chim. Acta* **1983**, *70*, 251.
(59) Fennema, B. D. J. R.; de Graaf, R. A. G.; Hage, R.; Haasnoot, J. G.; Reedjik, J.; Vos, J. G. *J. Chem. Soc., Dalton Trans.* **1991**, 1043.
(60) LaChance-Galang, K. J.; Doan, P.; Clarke, M. J.; Rao, U.; Yamano, A.; Hoffman, B. M. *J. Am. Chem. Soc.* **1995**, *117*, 3529.
(61) Mamo, A.; Stefio, I.; Poggi, A.; Tringali, C.; DiPietro, C.; Campagna, S. *New J. Chem.* **1997**, *21*, 1173.

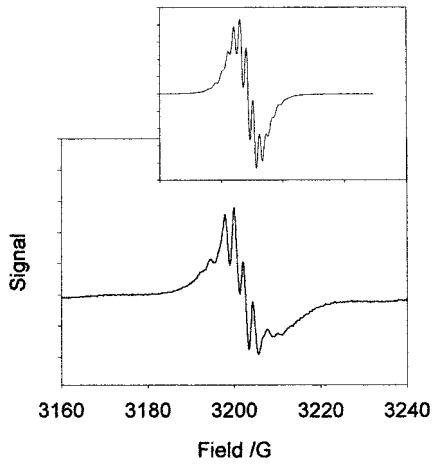


**Figure 3.** Experimental (lower) and simulated (upper inset) EPR spectra of complex 35−2H measured in methanol ($10^{-4}$ M NaOH).

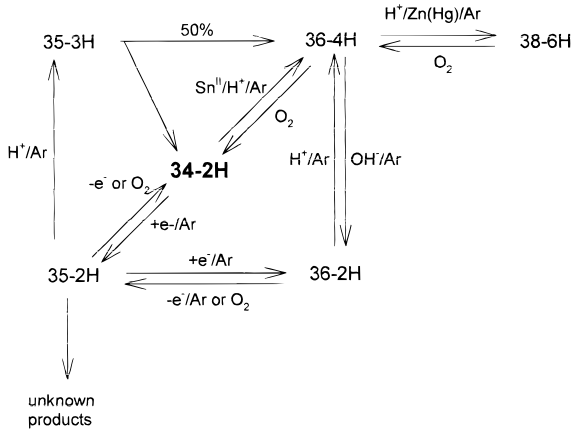


**Figure 4.** Interconversion routes connecting the complexes of LL in its various redox−proton states generated in methanol from complex [34−2H].

were based on comparisons with related systems.[38,62−64] The complex [34−2H] has a C═O stretch at 1667 $cm^{-1}$, a C═N stretch at 1584 $cm^{-1}$, and two C═C (cyclic alkene) stretching vibrations at 1529 and 1508 $cm^{-1}$ (structure 34−2H, Figure 1). The complex [36−4H] lacks the C═O stretch, preserves the C═N stretch at 1586 $cm^{-1}$, and has only one C═C (cyclic alkene) at 1506 $cm^{-1}$. The bands at 1604 $cm^{-1}$ in [34−2H] and 1600 $cm^{-1}$ in [36−4H] correspond to a bpy vibration. Structure D (Figure 2) of the [36−4H] complex is the isomer that best fits the previous assignments.

**3.3. EPR Spectrum of $[Ru(bpy)_2(35-2H)]^+$.** All the complexes under discussion are EPR silent except for [35−2H], obtained by the reduction of [34−2H] ($10^{-5}$ M complex in methanol containing 0.001 M NaOH), which displayed an EPR signal (g = 2.00) with the hyperfine structure shown in Figure 3. The seven line signal can be approximately simulated by assuming the following parameters: N(1) ($I = 1$, $A_N = 2.4$ G); N(2) ($I = 1$, $A_N = 2.2$ G); H(1,2) ($I = {}^1/_2$, $A_H = 2.5$ G); Ru ($I = {}^5/_2$, $A_{Ru} = 2.0$ G). Note that there are up to 10 inequivalent nuclei with $I \neq 0$ which may contribute to the hyperfine structure of this free radical.

The unpaired electron is in the [35−2H] orbital no. 105 (see section 4.0). Some delocalization onto the metal is revealed by the very weak satellite lines due to coupling to $^{101}$Ru (abundance 17.0%, $I = {}^5/_2$). The two nitrogen atoms involved in the coupling belong to the diiminoanthraquinone fragment and not the bipyridine units, but the hyperfine coupling to nitrogen is much smaller than that observed in the complex[11] $[Ru(bpy)_2(sqdi)]^+$ (sqdi = benzosemiquinone diimine) ($A_N$ = ca. 20 G).[11,12] This comparison provides evidence that reduction to the semiquinone involves primarily the para-quinone ring and, to a much lesser degree, the quinonediimine ring. The ROHF optimized structure of [35−2H] reveals some lengthening of the C═NH bond (Table 1).

**3.4. Interconversions.** The series of complexes and their assigned number of electrons and protons were deduced from a series of logical and consistent connections using optical spectroscopy as a principal guide to identity. Electrochemical oxidation and reduction tracked by coulometry allowed a count of the number of electrons involved in the interconversions. Chemically reduced or oxidized species in acidic or basic medium (protonation/deprotonation) were linked to the electrochemical products through their optical spectra.

The parent species [34−2H] was prepared as described[14] from $[Ru(bpy)_2Cl_2]$ and diaminoanthraquinone (DAAQ, ligand 36−4H). Two successive one-electron electrochemical reduction steps yield [35−2H] and [36−2H], respectively. Their electronic spectra were obtained by spectroelectrochemistry at a gold grid electrode. The processes are reversible as [36−2H] can be reoxidized by two electrons to recover [34−2H]. The species [34−2H] can be reduced in acidic methanol by stannous chloride to [36−4H]. On the other hand in methanolic sulfuric acid, reduction with zinc amalgam leads to [38−6H]. Air oxidation of [38−6H] in acidic medium leads first to [36−4H] and then finally to [34−2H]. In alkaline medium, air oxidation of [36−2H] leads to [35−2H], which subsequently decomposes to unknown products. The species [35−2H] can be obtained spontaneously by adding sodium hydroxide to a methanolic solution of [34−2H]. If this alkaline solution of [35−2H] is reacidified under argon, it generates the complex [35−3H], which disproportionates into a 50:50 mixture of [34−2H] and [36−4H]. Species [36−2H] and [36−4H] can be interconverted by addition of acid or base under an inert atmosphere. All of these interconversions were readily followed by electronic spectroscopy and are summarized in Figure 4.

## 4. ZINDO Calculations and Molecular Orbital Diagrams

**4.1. Free Ligand Frontier Orbitals.** The free ligand frontier orbital pictures (shown in Figure 6 for 34−2H) reveal that the LUMO and LUMO + 1, nos. 44 and 45, have the same symmetry with respect to the metal and are in-phase and out-of-phase combinations of the bqdi $\pi^*$ LUMO with a naphthoquinone $\pi^*$ orbital. In the local $C_{2v}$ symmetry of the bqdi fragment, with the $C_2(z)$ axis in the $(xz)$ plane of the quinone diimine ligand and bisecting the NRuN bond angle, as used in bqdi complexes,[7] these orbitals have $b_2$ symmetry, while HOMO − 1, no. 42, is $a_2$. The HOMO is a $\sigma$-orbital which is greatly stabilized upon coordination to ruthenium.

The energetically most favorable interaction between the metal $d(t_{2g})$ orbitals and the 34−2H (and also 35−2H, 36−2H, and 36−4H) ligand occurs if the orbitals are oriented at the Ru center according to this local $C_{2v}$ symmetry. The metal $d_{yz}$ orbital then interacts with $\pi$ symmetry potentially combining with $\pi$ or $\pi^*$ ligand orbitals of $b_2$ symmetry, while the $d_{xy}$ orbital of $a_2$

(62) Becker, E. D.; Charney, E.; Anno, T. *J. Chem. Phys.* **1965**, *42*, 942.
(63) Goss, C. A.; Abruna, H. D. *Inorg. Chem.* **1985**, *24*, 4263.
(64) Bellamy, L. J. *The Infrared of Complex molecules*, 2nd ed.; Chapman and Hall: London, 1980.

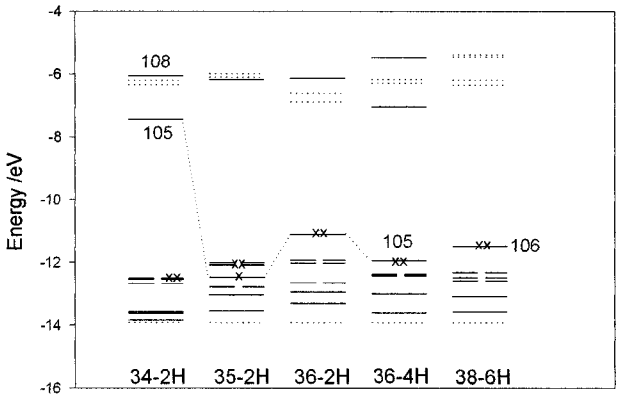


**Figure 5.** MO energies for the five $[Ru(bpy)_2(LL)]^{2+}$species as designated, derived from ZINDO/S calculations. HOMO and LUMO levels are identified. The dotted lines refer to bipyridine $\pi$-MO levels, and the dashed lines are mainly d-orbitals localized on the ruthenium center.

**Table 3.** Molecular Orbital Energies[a] of the Complexes $[Ru(bpy)_2(LL)]^{n+}$ (eV)

| MO no. | 34−2H | 35−2H[b] | 36−2H | 36−4H | 38−6H |
|---|---|---|---|---|---|
| 114 | −4.255 | −2.202 | 0.753 | −4.360 | −4.416 |
| 113 | −4.640 | −2.432 | 0.678 | −4.817 | −5.029 |
| 112 | −5.020 | −2.754 | −0.077 | −4.948 | −5.175 |
| 111 | −5.132 | −2.855 | −0.158 | −5.176 | −5.292 |
| 110 | −5.370 | −3.002 | −0.410 | −5.197 | −5.381 |
| 109 | −5.395 | −3.074 | −0.509 | −5.270 | −5.444 |
| 108 | −6.034 | −3.746 | −0.601 | −5.969 | −6.182 |
| 107 | −6.217 | −3.869 | −1.084 | −6.080 | −6.349 |
| 106 | −6.310 | −3.937 | −1.351 | −6.825 | −11.474 |
| 105 | −7.440 | −10.229 | −5.579 | −11.737 | −12.317 |
| 104 | −12.554 | −9.773 | −6.397 | −12.164 | −12.473 |
| 103 | −12.566 | −9.837 | −6.494 | −12.222 | −12.573 |
| 102 | −12.696 | −10.534 | −7.124 | −12.789 | −13.074 |
| 101 | −13.560 | −10.800 | −7.408 | −13.395 | −13.572 |
| 100 | −13.617 | −11.305 | −7.769 | −13.707 | −13.916 |
| 99 | −13.874 | −11.678 | −8.385 | −13.792 | −14.012 |
| 98 | −13.907 | −11.764 | −8.519 | −14.254 | −14.451 |
| 97 | −13.985 | −11.841 | −8.855[c] | −14.859 | −15.026 |

[a] Calculated using ZINDO/S; see text. [b] ROHF theory. [c] The highest filled bpy $\pi$-orbital is no. 96 at −8.964 eV.

symmetry would combine in a sideways $\delta$ sense with the appropriate ligand orbitals. The remaining $d(t_{2g})$ orbital will be $d_{x^2-z^2}$ and will have $\sigma$-symmetry with respect to LL. The remaining part of the LL ligand can be regarded as a naphthoquinone substituent which has the effect of increasing the number of $\pi$ and $\pi^*$ orbitals available for interaction with the ruthenium d orbitals and, of course, provides a mechanism for delocalization of charge. The two bpy ligands could reduce the apparent local symmetry from $C_{2v}$ to $C_2$, but evidently the interaction with the quinone diimine is sufficient to compensate.

**4.2. Orbital Energies and Mixing (Tables 3 and 4).** {See Web site, details below, for color pictures of the frontier orbitals of all the species under discussion.} The frontier molecular orbital energy level diagrams of the bis(bipyridine)ruthenium complexes containing the 34−2H, 35−2H, 36−2H, 36−4H−D, and 38−6H ligands are shown in Figure 5 with numerical data in Table 3. The open-shell $S = 0.5$ species was analyzed by restricted open-shell Hartree−Fock (ROHF) theory.

Because of the varying net charge on these complexes, the actual molecular orbital energies vary quite dramatically and cannot be readily compared on one diagram. To alleviate this problem the MO energies are normalized to the highest filled $\pi$ orbital on bpy. The two low-lying empty $\pi^*$ orbitals (nos. 44 and 45, Figure 6) on the 34−2H ligand are generally separated

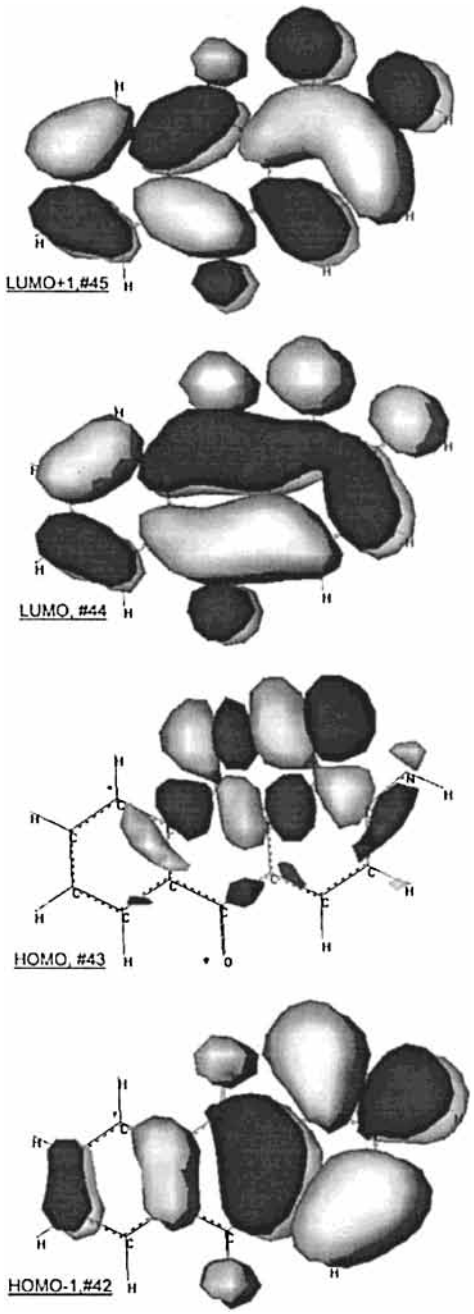


**Figure 6.** Free ligand frontier molecular orbitals for 34−2H. Reading down from the top are the following: LUMO + 1, no. 45; LUMO, no. 44; HOMO, no. 43 and HOMO − 1, no. 42. The coordinating ═NH groups lie in the top right corner. {A full color version of Figure 6 appears on our web site. Pictures of the frontier orbitals of free ligand 36−4H can also be found on our web site.}.

in energy from one another in the complexes by a pair of bpy-($\pi^*$) orbitals. Free ligand orbital no. 44 is primarily associated with no. 105 in complexes [34, 35, 36−2H] and no. 45 with no. 106 or no. 108 (Table 4).

Consider the data presented in Table 4. In all species, the $d(t_{2g})$ orbitals are mixed with both LL and bipyridine levels. While the Ru $d(t_{2g})$ set is largely localized on the metal in the [38−6H] (nos. 103−105) species, in the other species the Ru $d(t_{2g})$ orbital density contribute at least 10% to four to seven levels through mixing with ligand $\pi$ or $\pi^*$ orbitals of comparable energy. Specifically, these heavily mixed orbitals (cited in parentheses) are [34−2H] (nos. 102−105), [35−2H] (nos. 100−105), [36−2H] (nos. 100−105), and [36−4H] (nos. 102−105).

**Table 4.** Percentage Orbital Populations as a Function of Electron and Proton Count[a]

| | 38−6H | | | 36−4H | | | 36−2H | | | 35−2H | | | 34−2H | | |
|---|---|---|---|---|---|---|---|---|---|---|---|---|---|---|---|
| MO | Ru | bpy | LL | Ru | bpy | LL | Ru | bpy | LL | Ru | bpy | LL | Ru | bpy | LL |
| 108 | 7 | 93 | 0 | 6 | 93 | 1 | 2 | 22 | 76 | 6 | 94 | 1 | 5 | 8 | 87 |
| 107 | 3 | 97 | 0 L | 5 | 91 | 4 | 12 | 86 | 2 | 2 | 54 | 44 | 5 | 95 | 0 |
| 106 | 0 | 9 | 91 H | 9 | 8 | 82 L | 5 | 90 | 5 L | 1 | 43 | 57 L | 2 | 87 | 11 |
| 105 | 75 | 23 | 3 | 35 $\pi$ | 6 | 59 H | 18 $\pi$ | 7 | 75 H | 13 $\pi$ | 2 | 85 S | 18 $\pi$ | 6 | 77 L |
| 104 | 82 | 16 | 3 | 71 $\delta$ | 14 | 16 | 40 $\sigma$ | 24 | 37 | 43 $\delta$ | 11 | 46 | 68 $\delta$ | 10 | 22 H |
| 103 | 82 | 15 | 2 | 74 $\sigma$ | 22 | 4 | 62 $\delta$ | 8 | 30 | 42 $\sigma$ | 15 | 43 | 70 $\sigma$ | 19 | 11 |
| 102 | 1 | 0 | 99 | 28 $\pi$ | 9 | 63 | 50 $\pi$ | 15 | 34 | 54 $\pi$ | 18 | 28 | 56 $\pi$ | 12 | 32 |
| 101 | 0 | 20 | 79 | 6 $\delta$ | 4 | 90 | 38 $\sigma$ | 10 | 52 | 34 $\sigma$ | 14 | 52 | 0 | 0 | 99 |
| 100 | 1 | 98 | 1 | 1 | 98 | 1 | 14 $\delta$ | 5 | 81 | 23 $\delta$ | 17 | 60 | 4 $\delta$ | 2 | 95 |
| 99 | 2 | 98 | 0 | 2 | 97 | 1 | 0 | 0 | 100 | 1 | 98 | 1 | 5 | 29 | 66 |
| 98 | 0 | 4 | 95 | 1 | 2 | 96 | 0 | 0 | 100 | 3 | 90 | 7 | 1 | 96 | 3 |

[a] Ruthenium data contain small contributions from s and p orbitals but mostly reflect d orbital character. Data are rounded and may not always sum to 100%. H = HOMO, L = LUMO, and S = SOMO. $\delta$, $\sigma$, $\pi$ refer to approximate symmetry with respect to the LL ligand. The labels are least precise for the [35−2H] species.

All of these complexes have a local $RuN_6$ chromophore. The [34−2H], [36−2H], and [36−4H] species are all believed to contain a diimino fragment bound to ruthenium since the C═NH bond length remains short in the optimized structures (see Table 1 and further details on our Web site) and all possess a similar intense visible region absorption which, in all cases, contains a contribution from charge transfer to a diimine fragment (see below). However as the species are reduced, we can expect a build up of charge on the coordinating imine group which would possess some $NH^-$ character. Not surprisingly, the Mulliken charges do increase on both the ligating ═NH and the quinone oxygen (C═O) as the species are reduced. However, the C═NH bond distances (ZINDO optimized) are similar for [34−2H] and [36−2H] (Table 1) suggesting that both retain the quinonediimine structure. The C═NH bond length in [35−2H] is however longer, consistent with a contribution from a semiquinone canonical form.

The high-lying filled LL $\pi$-orbital no. 42 (Figure 6) mixes with the metal $d_{xy}$ ($d\delta$) orbital and is responsible for making this orbital shift to higher energy through (antibonding) destabilization (Table 3). Its admixture with ligand no. 42 is significant but less than the metal−ligand coupling of $d_{yz}$ (below). The corresponding bonding orbital is found at no. 100 in [34−2H], [35−2H], and [36−2H] but at no. 101 in [36−4H]. Mixing is least in [34−2H] and most in [36−2H] again likely because of the extra basicity of this formally dinegative (36−2H) ligand.

The $d_{yz}$ ($d\pi$) orbital has the correct symmetry to interact with either no. 44 or no. 45 and is lowest in energy (no. 102) through stabilization primarily (see Figure 7) by mixing with orbital no. 44 (see below). In species [34−2H] one can estimate a value for the Coulomb and exchange energies involved[65] in the $d_{yz}$ + (34−2H)$\pi^*$ → (34−2H) $\pi^*$-$d_{yz}$ transition. These are found to be $J$ = 33 560 and $K$ = 6400 $cm^{-1}$. The large value for $K$ is especially indicative of extensive mixing.[65]

Orbital no. 105 is the LUMO in [34−2H] and plainly results from an antibonding interaction of $d_{yz}$ with free ligand 34−2H no. 44 (LUMO). Orbital no. 105 is the SOMO in [35−2H] and the HOMO in both [36−2H] and [36−4H]. The Ru contribution to no. 105 increases slightly from species [34−35−36−2H] (ca. 20% back-bonding) and dramatically increases in [36−4H]. In both the [36−2H] and [36−4H] species, the $d_{yz}$ orbital interacts strongly with the free (34−2H) ligand $\pi^*$ orbital no. 44, in the pair of filled orbitals no. 102 and no. 105, respectively, in [36−2H], and in no. 105 in [36−4H]. The $d_{yz}$ orbital contribution to no. 102 is much smaller in [36−4H] compared with [36−2H], while the reverse is true for orbital no. 105 (see Table 4). Indeed the $d_{yz}$ orbital is most substantially delocalized in [36−4H].

Of especial interest is the extent of overall splitting of the filled d($t_{2g}$)-orbital set caused mainly by these interactions with the ligand LL. The magnitude of this splitting increases in the sequence of complexes [34−2H] (0.14 eV) < [35−2H] (0.76 eV (ROHF)) ≈ [36−2H] (0.73 eV) represented by the difference in energy between no. 104 and no. 102. This splitting is also large in [36−4H] (0.62 eV).

Thus mixing between filled LL($\pi$) levels and Ru d($t_{2g}$) becomes very important in these more electron rich [36−2H] and [36−4H] species. The latter case, for example (no. 102, LL($\pi$)), is some 30% localized on the metal. A color coded map of the fractional populations is available on our Web site (see details below). The frontier orbitals on [34−2H] and [36−2H] tend to localize on the quinonediimine fragment of the ligand while for [36−4H] there is greater delocalization over the whole ligand.

Complex [38−6H] involves a neutral non-$\pi$-bonding ligand since the Ru d levels are separated from the LL ligand $\pi$-network by the $-NH_2$ groups. Thus the d-orbitals here are calculated to be much purer than in the other species and LL contributions are very small. The HOMO (no. 106) is a pure ligand level with no Ru contribution. Orbital no. 105, the highest filled d orbital, has $\sigma$-symmetry with respect to the LL plane while the other two ZINDO-defined d($t_{2g}$) orbitals do not lie along the HN−Ru−NH bisector.

In these various species, back-donation into the bpy($\pi^*$) levels is much less than into LL($\pi^*$) being in the range 3−11% and involving the first and/or second lowest lying bpy($\pi^*$) level. Back-donation into bpy($\pi^*$) is usually calculated to be around 5% using ZINDO[65] or slightly greater using DFT.[66] The maximum value here of 12% (no. 107) occurs with the dinegatively charged 36−2H ligand due obviously to a more electron rich ruthenium center. Back-donation and mixing with the bpy($\pi^*$) levels in species [38−6H] occurs to an extent similar to that in the other complexes. In particular there is significant (7%) back-donation into orbital no. 108, the second bpy($\pi^*$) level.

**4.3. Spectroscopic Transitions and Assignments.** Table 5 summarizes the electronic transitions observed (Figure 8) with these various species, together with ZINDO/S predicted energies. In general we can anticipate MLCT transitions from Ru d($\pi t_{2g}$)

(65) Gorelsky, S. I.; Dodsworth, E. S.; Vlcek, A. A.; Lever A. B. P. *Coord. Chem. Rev.* **1998**, *174*, 469.

(66) Daul, C.; Baerends E. J.; Vernooijs, P. *Inorg. Chem.*, **1994**, *33*, 3538.

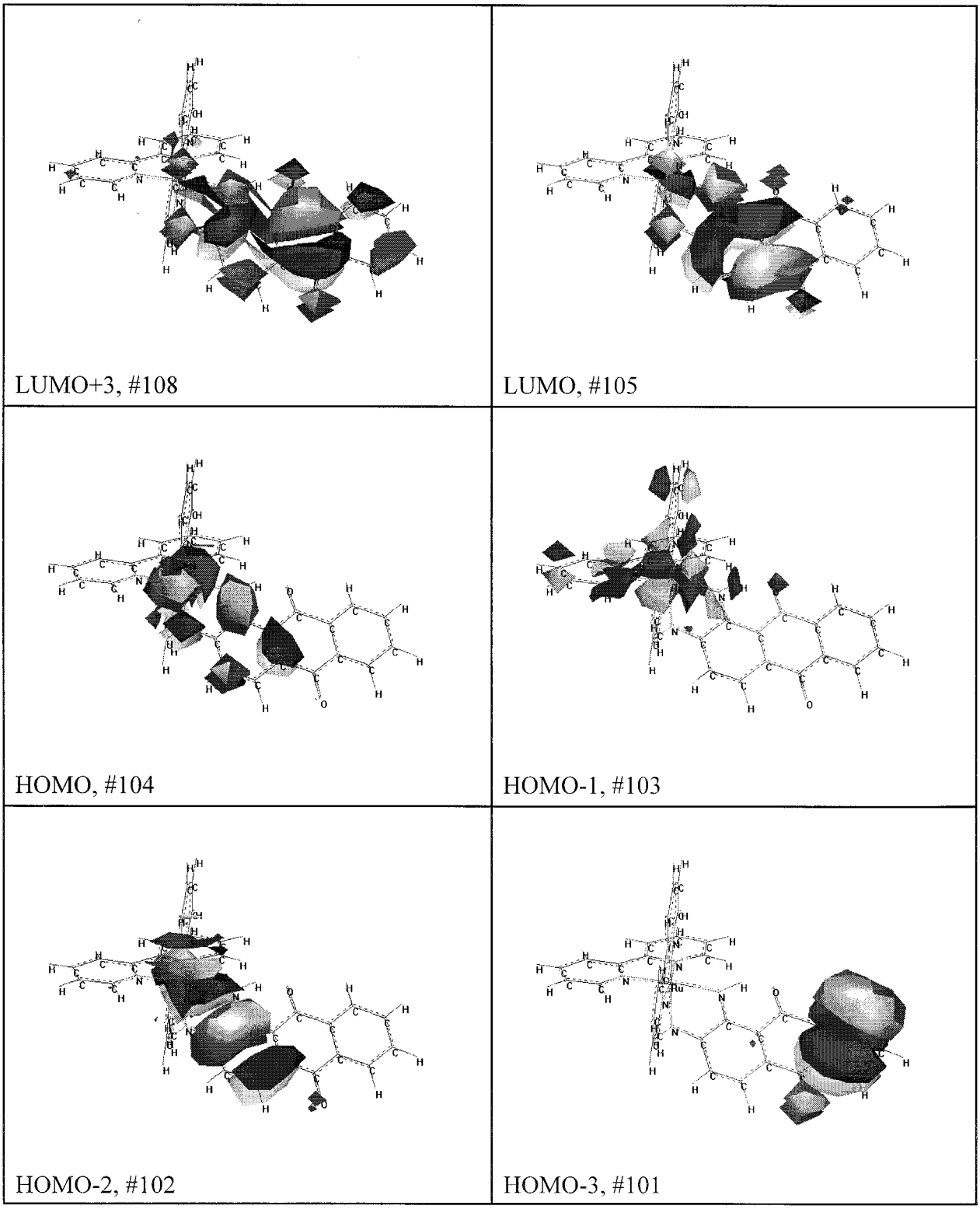


**Figure 7.** A selection of frontier molecular orbitals for complex [34−2H]. {Pictures of the frontier orbitals of other complexes described in this work can be found on our web site. A full color version of Figure 7 also appears on our web site.}

or d($\delta t_{2g}$) to LL($\pi^*$) and d($t_{2g}$) to bpy($\pi^*$) orbitals. The most intense MLCT transition (intensity ca. 20 000 L $M^{-1}$ $cm^{-1}$) is expected to be the transition between the bonding and antibonding combinations of $d_{yz}$ (d$\pi$) and LL($\pi^*_1$) (no. 105). This should be at relatively high energy since $d_{yz}$ is stabilized and there will be a fairly large ($-J + 2K$) contribution to this transition because of extensive mixing.[65,67] This transition can only be observed in the complexes [34−2H] and [35−2H] since the terminating orbital is filled in the other complexes. However there is a higher lying LL($\pi^*_2$) orbital, no. 106 or 108 in the various complexes (Table 4), and MLCT transitions terminating on this orbital can be expected in all the complexes except [38−6H]. Moreover, since LL($\pi^*$) levels are being filled from [35−2H] to [36−4H], we can also expect internal LL ligand $\pi^* \rightarrow \pi^*$ transitions with MLCT character (no. 105 → no. 106) and

(67) Shin, Y. K.; Brunschwig, B. S.; Creutz, C.; Newton, M. D.; Sutin, N. *J. Phys. Chem*. **1996**, *100,* 1104.

**Table 5.** Spectroscopic Data for $[Ru(bpy)(LL)]^{n+}$ Complexes in Methanol

| LL | expt. data[a] | calcd data[b] | assignments |
|---|---|---|---|
| 34−2H | 10 900 (0.2) | 9 150 {0.002} | [103, 104 → 105] $d_{x^2-z^2}$,$d_{xy}$ → 34−2H($\pi^*$) − $d_{yz}$ |
| | 17 900 (22.2) | 18 300 {0.05} | [99 → 105] 34−2H($\pi$) → 34−2H($\pi^*$) − $d_{yz}$ |
| | | 18 900 {0.6} | [102 → 105] $d_{yz}$ + 34−2H($\pi^*$) → 34−2H($\pi^*$) − $d_{yz}$ |
| | 23 900 (6.6) | 23 100 {0.13} | [103, 104 → 106] d + 34−2H($\pi$) + bpy($\pi$) → bpy($\pi^*_1$) |
| | 26 600 (7.6) | 24 600 {0.06} | [100 → 105] bpy($\pi$) → 34−2H($\pi^*$) − d |
| | | 25 700 {0.05} | [102 → 107]$d_{yz}$ + 34−2H($\pi$) → bpy($\pi^*_1$) |
| | | 27 400 {0.15} | [101 → 105] 34−2H($\pi$) → 34−2H($\pi^*$) − d |
| | | 30 000 {0.17} | [104 → 108] $d_{xy}$ → 34−2H($\pi^*$) |
| | 35 000 (46.0) | 30 600 {0.1} | [97 → 105] bpy($\pi$) → 34−2H($\pi^*$) |
| | | 31 800 {0.11} | [103 → 109, 110] $d_{x^2-z^2}$ → bpy($\pi^*_2$) |
| | | 32 700 {0.06} | [104 → 109] $d_{xy}$ → bpy($\pi^*_2$) |
| | | 33 000 {0.19} | [103 → 110] $d_{x^2-z^2}$ → bpy($\pi^*_2$) |
| | | 33 100 {0.16} | [103 → 109] $d_{x^2-z^2}$ → bpy($\pi^*_2$) |
| | | 33 900 {0.1} | [103 → 111][102 → 109] d → bpy($\pi^*_2$) |
| | | 34 700 {0.05} | [102 → 110] $d_{yz}$ → bpy($\pi^*$) |
| | | 36 000 {0.68} | [103, 104 → 111] d → bpy($\pi^*$) |
| | | 36 200 {0.16} | [103, 104 → 112] d→ bpy($\pi^*$) |
| | | etc. | |
| | 41 700 (50.5) | | |
| 35−2H | 9 700 (8.3) | 6 400 {0.0005} | [101, 103 → 105] d → 35−2H($\pi^*$) − d |
| | 11 100 (2.9) | | |
| | 13 600 (27.2) | 12 060 {0.06} | [104 → 105] d − 35−2H($\pi$) → 35−2H($\pi^*$) − d |
| | | | [105 → 106, 107] 35−2H($\pi^*$) − d → 35−2H($\pi^*$) |
| | 14 500 sh | 14 450 {0.05} | [104 → 105] d→ ($\pi^*$) − d; [105 → 106] 35−2H($\pi^*$) − d → 35−2H($\pi^*$) |
| | 20 500 (7.9) | 19 600 {0.16} | [102 → 105] d + 35−2H($\pi^*$) → 35−2H($\pi^*$) − d |
| | 22 700 sh | 20 150 {0.03} | [103, 104 → 108] d → bpy($\pi^*_1$) |
| | | 21 400 {0.07} | [104 → 107] various d → ($\pi^*$) 35−2H, bpy |
| | | 21 500 {0.05} | [101, 103 → 105] |
| | | 21 700 {0.09} | [104 → 106, 107] |
| | | etc.[d] | |
| | 28 200 (14.3) | 27 500 {0.05} | [105 → 114] 35−2H($\pi^*$) − d → bpy($\pi^*_2$) |
| | | etc. | |
| 36−2H | 13 100 (27.7) | 11 500 {0.05} | [105 → 106] 36−2H($\pi^*$) − $d_{yz}$ → bpy($\pi^*_1$) |
| | | 12 200 {0.05} | [105 → 107] 36−2H($\pi^*$) − $d_{yz}$ → bpy($\pi^*_1$) |
| | 14 300 sh | 14 950 {0.11} | [104 → 106] d → bpy($\pi^*_1$) |
| | 16 700 (4.6)[c] | 15 600 {0.24} | [104 → 106] |
| | | 17 000 {0.39} | [104 → 107] d → bpy($\pi^*_1$) |
| | 20 500 (8.8) | 18 600 {0.25} | [105 → 108] 36−2H($\pi^*$) − $d_{yz}$ → 36−2H($\pi^*$) |
| | | 19 500 {0.08} | [105 → 109, 110] 36−2H($\pi^*$) − $d_{yz}$ → bpy($\pi^*_2$) |
| | | 19 700 {0.05} | [105 → 109, 110] 36−2H($\pi^*$) − $d_{yz}$ → bpy($\pi^*_2$) |
| | | 21 800 {0.03} | [103 → 108] d → 36−2H($\pi^*$) |
| | | 22 700 {0.07} | [103 → 109][105 → 112] d → bpy($\pi^*$) |
| | | 23 100 {0.06} | |
| | 27 900 (14.9) | | [103 → 110] |
| | | etc. | |
| 36−4H | n.o. | 12 500 {0.004} | [103, 104 → 6] d$\sigma$,$\pi$ → 36−4H($\pi^*$) − $d_{yz}$ |
| | 16 000 (27.6) | 16 000 {0.75} | [105 → 106] d − 36−4H($\pi$) → 36−4H($\pi^*$) − d |
| | 17 000 sh | | vibrational component? |
| | 21 800 (11.9) | 21 800 {0.15} | [105 → 108] 36−4H($\pi$) − d → bpy($\pi^*$); [103 → 107] d → bpy($\pi^*_1$) |
| | 24 800 (11.4) | 23 300 {0.07} | [102 → 106] 36−4H($\pi$) + d → 36−4H($\pi^*$) − d |
| | 26 800 (12.4) | 29 500 {0.07} | [105 → 109] d − 36−4H($\pi$) − d → bpy($\pi^*_2$) |
| | 31 200 (10.8)[c] | 31 400 {0.22} | many |
| | | 31 800 {0.18} | [103 → 112] d → bpy($\pi^*$) |
| | 34 500 (53.4) | 33 900 {0.26} | many |
| | | 34 200 {0.07} | [104 → 113] d → bpy($\pi^*$) |
| | | 34 900 {0.41} | [99 → 106] bpy($\pi$) → 36−4H($\pi^*$) |
| | | 35 300 {0.13} | [103 → 113] d + bpy($\pi$) → bpy($\pi^*$) |
| | | etc. | |
| 38−6H | 20 400 (9.6) | 19 600 {0.03} | [105 → 107] → bpy($\pi^*_1$) |
| | 23 100 (9.0) | 21 500 {0.15} | [103 → 107][104 → 108] d → bpy($\pi^*_1$) |
| | | 23 900 {0.05} | [105 → 108] d → bpy($\pi^*_1$) |
| | 26 200 (11.7) | 25 500 {0.17} | [106 → 111] $\pi$ → 38−6H($\pi^*$) |
| | 27 600 (11.6) | 26 900 {0.12} | [106 → 114][102 → 111] $\pi$ → 38−6H($\pi^*$) |
| | | 28 900 {0.09} | [105 → 109] d → bpy($\pi^*_2$) |

[a] Energy data in wavenumbers, $cm^{-1}$, with molar absorptivity in parentheses ($\epsilon/10^3$ L $mol^{-1}$ $cm^{-2}$); n.o. = not observed, sh = shoulder. [b] Oscillator strengths shown in braces. Calculated transitions with oscillator strengths < ca. 0.05 are generally not listed. [c] Gaussian deconvoluted component. [d] Many weak features.

possibly LL($\pi^*$) to bpy($\pi^*$) transitions (mediated through overlap with Ru d orbitals).

Reduction and protonation of [36−4H] generating [38−6H] breaks the conjugation between the ligand LL and the metal. The spectrum of complex [38−6H] should display internal anthraquinone and bands similar to those of[68] $[Ru(bpy)_2(NH_3)_2]^{2+}$.

All complexes are $Ru^{II}$ species and should display[65,68−74] two

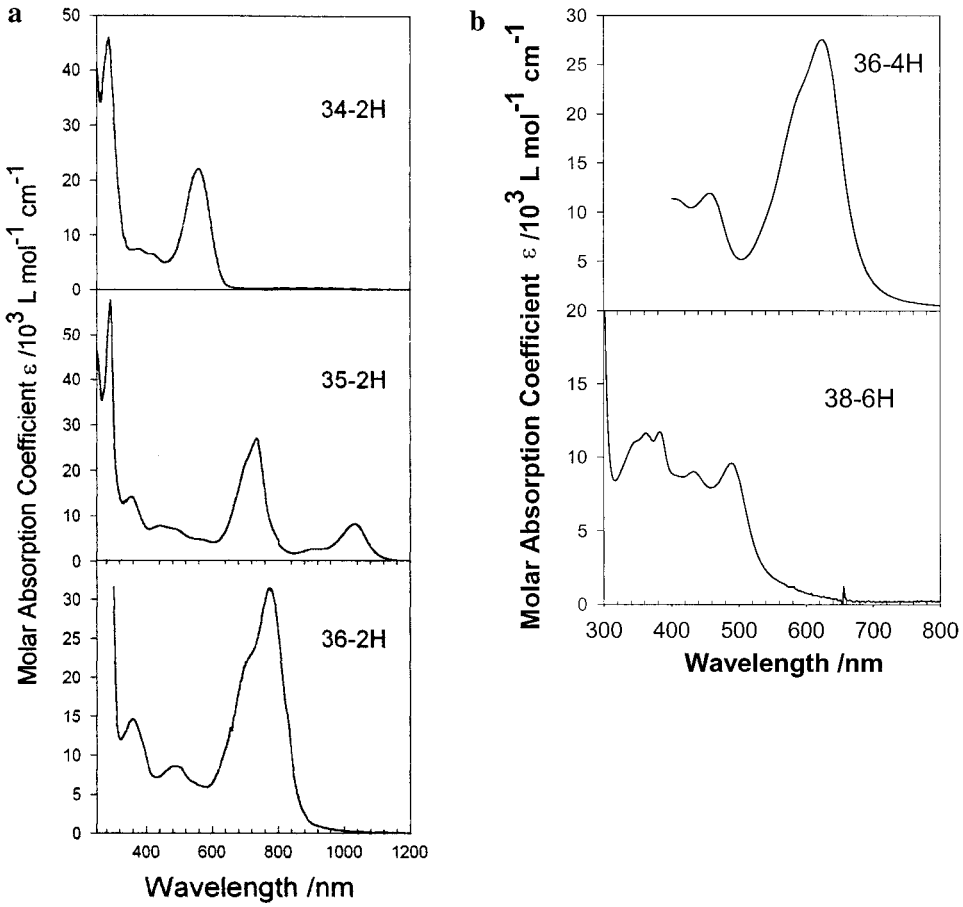


**Figure 8.** UV/vis electronic absorption spectra of the complexes in methanol: (a) $[Ru(bpy)_2(34-2H)]^{2+}$, $[Ru(bpy)_2(35-2H)]^{+}$, and $[Ru(bpy)_2(36-2H)]$; (b) $[Ru(bpy)_2(36-4H)]^{2+}$ and $[Ru(bpy)_2(38-6H)]^{2+}$.

Ru to bpy transitions, separated by some 7000−8000 $cm^{-1}$. The UV bands with intensities of 40 000 L $mol^{-1}cm^{-1}$ are expected due to $\pi$ to $\pi^*$ transitions of the ligands LL and bpy. The four species [34−2H], [35−2H], [36−2H], and [36−4H] all have rather similar absorption in the visible region with strong bands of molar intensity near 20 000 L $mol^{-1}$ $cm^{-1}$. According to the ZINDO calculations these are all assigned to $d\pi \rightarrow LL(\pi^*)$ transitions but with varying contributions from $\pi \rightarrow \pi^*$ internal to the ligand.

The spectra have all been subject to Gaussian deconvolution, and the results are shown in Figure S5. However because of the uncertainty in defining the number of Gaussian bands, we use the raw undeconvoluted data in Table 5 except where ZINDO predicts a band which is "observed" in the Gaussian analysis but which is not seen as a separate band in the original spectrum.

**4.3.1. $[Ru(bpy)_2(34-2H)]^{2+}$.** The lowest energy band should be the HOMO (no. 104) to LUMO (no. 105), $d_{xy} \rightarrow (34-2H)(\pi_1^*)$ band. Indeed a pair of bands are predicted with extremely low intensity[65] assigned to this transition mixed and to the $\sigma(t_{2g}) \rightarrow LL(\pi^*_1)$ transition. These correspond with a very weak experimental band with an intensity of about $1 \times 10^2$ L $mol^{-1}$ $cm^{-1}$. The appearance of these weak MLCT type transitions to the red of the intense MLCT band ([102 → 105]) has previously been discussed.[65,67]

The strongest feature in the spectrum is indeed the anticipated $d_{yz} + 34-2H(\pi^*) \rightarrow 34-2H(\pi^*) - d_{yz}$ [no. 102 → no. 105] transition, but there is also a predicted weak shoulder which is in fact an internal 34−2H transition [no. 99 → no. 105] (Table 5). This is followed by a $d \rightarrow bpy(\pi^*)$ transition and then by a succession of bands as noted in Table 5. The agreement between experimental and predicted energies is exceptionally good.

**4.3.2. $[Ru(bpy)_2(35-2H)]^{+}$.** The SOMO is no. 105 and is located on the ligand LL which is now effectively a semiquinonediimine. This orbital contains a significant contribution from $d_{yz}$ and lies fairly close in energy to the filled $d(t_{2g})$ orbitals. Thus the low-lying weak near-infrared bands are surely assigned as $d \rightarrow$ SOMO. ZINDO/ROHF predicts this assignment but at a rather lower energy (and lower intensity) than observed experimentally (Table 5). The remaining transitions are reasonably predicted by ZINDO/ROHF to be $Ru(d) \rightarrow 35-2H(\pi^*)$ and $Ru(d) \rightarrow bpy(\pi^*)$ (Table 5), and agreement with experiment is fairly good. As anticipated, the extra charge on the 35−2H ligand relative to 34−2H shifts the first $Ru(d) \rightarrow bpy(\pi^*)$ band to lower energy in [35−2H] than in [34−2H] (Table 5).

**4.3.3. $[Ru(bpy)_2(36-2H)]$.** The agreement between observed and predicted transition energies for this species is quite reasonable. The lowest energy feature near 13 000 $cm^{-1}$ should be the HOMO → LUMO transition, and this is so predicted by the ZINDO/S calculation. However ZINDO/S shows that this

(68) Juris, A.; Balzani, V.; Barigelletti, F.; Campagna, S.; Belser, P.; von Zelewsky, A. *Coord. Chem. Rev.* **1988**, *84*, 88.
(69) Luo, Y.; Potvin, P. G.; Tse, Y.-H.; Lever, A. B. P. *Inorg. Chem.* **1996**, *34*, 5445.
(70) Noble, B.; Peacock, R. D. *Inorg. Chem.* **1996**, *35*, 1616.
(71) Ohsawa, Y.; Hanck, K. W.; DeArmond, M. K. *J. Electroanal. Chem.* **1984**, *175*, 229.
(72) Krausz, E.; Ferguson, J. *Prog. Inorg. Chem.* **1988**, *37*, 293.
(73) Tait, C. D.; Donohoe, R. J.; DeArmond, M. K.; Wertz, D. W. *Inorg. Chem.* **1987**, *26*, 2754.
(74) Lever, A. B. P. *Inorganic Electronic Spectroscopy*, 2nd ed.; Elsevier Science Publ.: New York, 1984.

transition is mainly 36−2H($\pi$*) → bpy($\pi$*) character, and if this is so, it is rather surprising that the experimentally observed band is so narrow since an appreciable reorganization energy would be anticipated. Resonance Raman spectroscopy will be required to confirm this assignment.

The ruthenium is even more electron rich in this species compared with [34−2H] and [35−2H] so the Ru(d) → (bpy) $\pi$* transitions have now moved to quite low energy and appear before the first intense Ru(d) → 36−2H($\pi$*) transition (no. 105 → 108, Table 5). The second Ru(d) → bpy($\pi_2$*) has also moved to relatively low energy. The spectrum is quite complex so that resonance Raman spectroscopy will be sought to confirm these assignments.

**4.3.4. $[Ru(bpy)_2(36-4H)]^{2+}$.** The HOMO again is mixed-metal $d_{yz}$ and ligand $\pi$*. Agreement between observed and predicted spectroscopic energies is excellent for this species. The most intense band both observed and predicted at 16 000 $cm^{-1}$ is analogous to the first strong band in the [36−2H] species being an internal $\pi^* \rightarrow \pi^*$ (36−4H) transition with significant Ru content. The next main feature at 21 800 $cm^{-1}$ (calculated 21 800 $cm^{-1}$) is HOMO → bpy($\pi^*_1$) occurring at somewhat higher energy than the corresponding band in [36−2H] due to the extra positive charge. Higher energy bands are ascribed (Table 5) to MLCT type transitions to higher $\pi$* levels of [36−4H] and bpy. Again the spectrum is dominated by $d_{yz} + \pi^* \rightarrow \pi^* - d_{yz}$ type transitions. The anticipated Ru($d_{xy}$) → 36−4H($\pi$*) transition is predicted to be very weak and lie at low energy (calcd 12 500 $cm^{-1}$). It was not observed experimentally.

**4.3.5. $[Ru(bpy)_2(38-6H)]^{2+}$.** Agreement between observed and predicted spectra is very reasonable. The low-energy region should be, and is, dominated by MLCT to bpy($\pi$*) transitions. At slightly higher energies arise $\pi-\pi^*$ (38−6H) bands. There are no low-lying MLCT to (38−6H) since this is fully reduced to the diamine/hydroquinone oxidation level.

## 5. Summary and Conclusions

All complexes $[Ru(bpy)_2(LL)]^{n+}$ (LL = 35−2H, 36−2H, 36−4H) generated in methanol can be quantitatively reconverted into $[Ru(bpy)_2(34-2H)]^{2+}$ by acidification and subsequent exposure to air or oxygen. The existence of cycles coupling these redox−proton states suggests that an investigation of the nature of the products of oxygen reduction would be useful. It is possible that the oxidation of complex $[Ru(bpy)_2(36-4H)]^{2+}$ to $[Ru(bpy)_2(34-2H)]^{2+}$ produces hydrogen peroxide in analogy with the action of the industrial catalyst 2-ethylanthraquinone.[75] The possibility of modifying existing organic catalysts with metal complexes is intriguing and might be the answer to problems that cannot be solved with organic substituents. The existence of robust complexes such as $[Ru(bpy)_2(34-2H)]^{2+}$ is certainly a stimulus for this area of research.

The generally very good agreement between the experimental electronic spectra and the spectra predicted by ZINDO/S analyses provides assurance that the view of these species as described by their orbital energies and orbital mixing is reliable. The very extensive delocalization is a dominant feature of these species, increasing with the electron richness of the ligand. Not only is back-donation to empty LL($\pi$*) orbitals very important but mixing between Ru ($d(t_{2g})$) and filled LL($\pi$) orbitals also plays a major role in the more electron rich species [36−2H] and especially [36−4H].

The extent of $\pi$-back-donation/$\pi$*-mixing into the diimino-anthraquinone ligand is approximately the same in [34, 35, and 36−2H] as illustrated by the Ru content of orbital no. 105 (Table 5), and this occurs despite the increasing net charge on the LL ligand. The phenomenon can be understood in terms of a synergistic interaction in which the increasingly negatively charged ligand transfers electron density to the Ru center, by a $\sigma$-mechanism, making it more electron rich. One also observes greater mixing between filled d and filled ligand $\pi$-orbitals in this same sequence because these $\pi$-orbitals are more readily polarizable. The coefficients in Table 4 further demonstrate that the primary mechanism for delocalization in the dinegative (36−2H) ligand complex is $\sigma$ since the contribution of the $t_{2g}(\sigma)$ orbital is split over orbitals no. 101 and no. 104. This is clearly different from the primary $\pi$ mechanism seen with [34−2H] and [36−4H] where it is the $t_{2g}(\pi)$ orbital which is predominantly shared over two or more orbitals. In [35−2H] all types of orbital are coupled strongly to ligand orbitals, there being no $t_{2g}$ orbital more than 54% pure.

The systems behave somewhat like delocalized organic molecules with the Ru atom an integral part of the delocalization pathway. The possibility of using these fragments as components of a molecular wire is being explored.

**Acknowledgment.** We thank Sergei I. Gorelsky, and Drs. Hitoshi Masui, Scott Fielder, Vladimir Strelets, Antonin Vlcek, Yuhong Tse, Jiujun Zhang, William J. Pietro, Douglas N. Butler, Roberto da Silva, and Antonietta DelMedico for their intellectual and/or practical help. We gratefully acknowledge the loan of $RuCl_3$ from the Johnson Matthey Corp. We also thank York University and UFPR Brazil for financial aid to C.J. d.C.

**Supporting Information Available:** Figures and tables providing spectra and spectral data. This material is available free of charge via the Internet at http://pubs.acs.org. Additional information and color versions of some of the figures can be found on our Web site at: www.chem.yorku.ca/profs/lever/blever.htm following the links to this paper.

IC9905594

(75) Crampton, C. A.; Faber, G.; Jones, R.; Leaver J. P.; Schelle, S. *The Modern Inorganic Chemicals Industry*; Thompson, R., Ed.; Chemical Society Special Publications: London, 1977; No. 31.